J. Civil Eng. Mater.App. 2020 (December); 4(4): 223-232

Journal of Civil Engineering and Materials Application

Journal home page: http://jcema.com

Received: 23 September 2020 • Accepted: 15 November 2020

Research

doi: 10.22034/JCEMA.2020.245947.1039

Quasi-Static and Dynamic Analysis of Vertical and Horizontal Displacements in Earth Dams (Case Study: Azadi Earth Dam)

Ahmad Reza Mazaheri, Mostafa Zeinolebadi Rozbahani, Behrang Beiranvand *

Water Engineering and Hydraulic Structures, Department of Civil Engineering, Faculty of Engineering, University of Ayatollah Ozma Borujerdi, Borujerd, Iran.

Correspondence should be addressed to Behrang Beiranvand, Faculty of Engineering, Department of Civil Engineering, Water Engineering and Hydraulic Structure, University of Ayatollah Ozma Borujerdi, Borujerd, Iran. Tel: +986633231711, Fax: +980663323171; Email: ehrang220@gmail.com

ABSTRACT

Seismic analysis of earth and rockfill dams is generally done in two ways: quasi-static and dynamic. However, a quasi-static method with easy application and simple assumptions may lead to unsafe and uneconomical results. In the present study, two static and dynamic analyzes have been used nonlinearly using the Rayleigh Damping rule to calculate the settlement and horizontal displacement of Azadi Dam in the stages of the end of construction and steady-state seepage. Also, in numerical analysis, Abaqus software and a simple elastoplastic behavior model based on the Mohr-Coulomb criterion have been used. The seismic analysis results show that settlement is more sensitive to horizontal displacement, so that settlement at the upper, middle, and lower levels of the shell is 66%, 55%, and 52% more than horizontal displacement, respectively. The highest amount of settlement occurred in both quasi-static and dynamic states in the dam's upper levels, with the difference that in the dynamic state and the full reservoir, the upstream shell is more affected by settlement. Also, settlement in the dynamic analysis is 37% higher than the quasi-static analysis.

Keywords: **Abaqus, quasi-static analysis, dynamic analysis, settlement, horizontal displacement**

1. INTRODUCTION

Seismic design and analysis of earth and rockfill dams are done by two methods, quasi-static and dynamic. The method of dynamic analysis is mainly based on stress analysis and displacement, which is usually done with the help of finite element methods. This method is commonly used to analyze the stability of large dams in the study phase. Lack of accurate software for dynamic analysis of earth dams, the limited number of experts aware of dynamic analysis, the complexity of dynamic analysis method, expensive tests for determining soil dynamic properties, frequency, and ease of analysis with quasi-static software are the reasons for widespread use of the quasi-static method. Due to these cases, determining the accuracy of the quasi-static method and creating a relationship between the solutions of the two quasi-static and dynamic methods is of interest to earth and gravel dam design engineers. Today, the development of finite element and finite difference software has made it possible to use dynamic analysis as well as quasi-static analysis. Ambraseys and Sarma, 1967examined the response of earth dams to several earthquakes [1]. They calculated the time history and distribution of earthquake acceleration in the dam body. (Sarma, 1975) developed diagrams for calculating the critical horizontal acceleration in which the critical horizontal acceleration is the acceleration that can bring the soil mass limited to a landslide level into equilibrium [2]. (Tsai et al., 2006) by studying the dynamic response of the Pao-Shan dam, studied the effect of core dimensions on the potential of earth dam response as well as the effect of core width and height ratio and dam length and height ratio at the first natural frequency [3]. (Tsompanakis et al., 2009) Using a neural network, evaluated the dynamic response of the sample embankment (laboratory) using the finite element method. Considering the nonlinear behavior of soil materials, he concluded that the magnification module would shrink as the maximum earthquake acceleration increases and the materials enter the nonlinear section [4]. (Elia et al., 2011), investigated the seismic and aftershock

behavior of the Marana homogeneous dam in Italy [5]. (Mukherjee, 2013) The basic concepts of different methods of seismic stability analysis of earth dams along with salient features, advantages, and limitations of each. To realistically predict the earth dam response during an earthquake, the factors of nonlinear soil elastic behavior, the dependence of the enclosed soil pressure on its stiffness, the geometry of the valley, and the intersection of the dam with the alluvium must be carefully considered [6]. (Huang, 2014) analyzed the seismic response of earth dams with stabilizing materials (materials with low strength control, CLSM) using the finite element method. Their results show that the use of CLSM is suitable for stabilizing embankments against seismic excitation [7]. According to studies (Panulinova and Harabinova, 2014), the stability of earth dams against landslides or seismic effects should be designed in such a way that the embankment is not destroyed due to changes in soil properties or external influences and remains stable [8]. (Bandini et al., 2015) presented a limit equilibrium model in which changes in block geometry, as well as changes in shear strength due to slip, are considered. He compared the results of observational models with the results of numerical analysis [9]. In all these comparisons, the observed behavior is consistent with the predicted one, which indicates the need to take into account the block geometry change and the shear strength due to shear in the calculations. Luo et al. (2018) examined the Chengbehi dam monitoring in 18 years using piezometric pressure and settlement results and found that the maximum dam in the middle of the dam was 178 mm, which gradually decreased from the middle to the sides [10]. Sukkarak and Jongpradist (2019), in their study of settlement rockfill dams, found that the geometry of the dam is very important, especially in narrow valleys in terms of the settlement. During impounding and operation, the dam body withstands all internal and external loads [11]. This often causes horizontal and vertical displacements, called vertical settlement locations (Ik-Soo, 2011) [12]. In another study by Rashidi et al. (2018) by examining and comparing the results of the instrumentation of the Siah Sang dam and numerical analysis using the Mohr-Coulomb model, it showed that the study dam is safer in terms of hydraulic failure at the end of construction and the first impounding period compared to other rockfill dams in the world. Although major displacements occur during the construction of the dam, the study of the earth dam's settlement sometimes leads to effective results [13]. In general, the maximum settlement of the dam is in its midpoints and gradually decreases until it reaches zero in the paws. Because of the settlement, the structure of the dam gradually stretched, and the distance between the tiller's slopes along the base slightly increases (Gikas and Sakellario, 2008). Silvani et al. (2006) used a Distinct Element Method (DEM) to investigate the effects of buoyancy forces and the decrease in the coefficient of friction in a rockfill column [14,15]. In a separate study, Karalar et al. (2017–2020) analyzed the numerical analysis of earth dams [16-19]. In this study, quasi-static and dynamic analysis of vertical and horizontal displacements of Azadi earth dam using Abaqus software and nonlinear analysis have been investigated and compared.

2. MATERIALS AND METHODS

2.1. GEOGRAPHICAL LOCATION AND GEOLOGY OF AZADI DAM

Azadi Reservoir Dam is located in Iran and Kermanshah province, 500 m downstream of Shahgozar Bridge, and about 90 km from Javanrood city in the coordinates of 46`21 east longitude and 34`33 north latitude on Zamkan River. The catchment area of this river up to the axis of Azadi Dam is 1054 km2. Access to Azadi Reservoir Dam is possible through Kermanshah Road, Kuzran-Shahgozar Bridge. Azadi Dam is a rockfill type with clay core with a height of 64 m from the foundation to 1312 (masl) meters above sea level and a crest length of 737 m. The volume of the dam reservoir at the normal level is 57.47 million m3, and the useful volume is 50 million m3 (Figure 1).

Figure 1. Azadi earth dam, Kermanshah, Iran

Azadi Reservoir Dam site consists of two rocky sections of Chilean Amiran sediments and marl limestone of Gurpi Formation and the alluvial-debris sediment unit of the present period in the right-axis ridge and under the overflow. In terms of geostructure, the Azadi Dam area and related facilities belong to the folded Zagros structural unit in East Lorestan. This structural unit, like other folded Zagros regions in the south and southwest of Iran, has a stressful past in terms of tectonic activity. Of course, in this area, folding and faulting of formations are normal and natural (Abdan Faraz Consulting Engineers). Azadi Reservoir Dam site is composed of two rock sections: Amiran Formation shale sediments - Gurpi Formation

marl limestone and alluvial-debris sediments of the present era in the right-axis and below the overflow. In terms of geostructure, the area of Azadi Dam and related facilities belong to the Zagros fold and thrust belt structural unit (Zagros FTB) in East Lorestan. This structural unit, like other Zagros FTB areas in the south and southwest of Iran, has had many tectonic activities in the past. Of course, in this area, folds and faults of the formations are normal (Abdan Faraz Consulting Engineers) [20].

2.2. GOVERNING EQUATIONS FOR STRUCTURAL DYNAMICS

By discretizing the dynamic equation of the structure and considering the applied forces of the earthquake in the time domain and using the finite element approach, the dynamic equation governing the dam and foundation will be written in matrix form (1):

$$[M]\{U^{\cdot\cdot}\} + [C]\{U^{\cdot}\} + [K]\{U\} = \{F_1\} - [M]\{U_g\} + [Q]\{P\} \quad (1)$$

[M], [C], and [K] are the matrices of mass, damping, and stiffness of the structure, respectively. $\{U\},\{U^{\cdot}\},\{U^{\cdot\cdot}\}$, $\{F_1\}$ and $\{U_g\}$ are the relocation, velocity, structural acceleration, body forces, and earthquake acceleration, respectively.

2.2.1. Complete Elastoplastic Analysis Of Embankment Assuming Mohr-Coulomb Theory

In an elastic-plastic analysis (complete plastic), the beginning of the stress-strain curve is linear, and its plastic range is linear. A yield function must be defined to evaluate whether the point has reached the plastic limit. Yield Criterion is usually expressed in terms of principal stresses or stress tensor variables. The onset of the condition is determined by the surrender criteria. The general form of the Yield Criterion can be given as Equation (2).

$$F = f(\sigma_1, \sigma_2, \sigma_3, n_1, n_2, n_3) \quad (2)$$

n_i show the direction of the main stresses σ_i. If the materials are the same, the Yield Criterion becomes a simple equation (3):

$$F = f(\sigma_1, \sigma_2, \sigma_3) \quad (3)$$

If the stress field is such that F (σ) <0 is the behavior of the elastic material and as soon as the yield point 0 = F (σ) is reached, the plastic behavior of the material begins. In the complete elastic model, the strain diagram consists of two components, elastic and plastic (Equation 4):

$$d\varepsilon = d\varepsilon^e + d\varepsilon^p \quad (4)$$

For plastic strains, the law of flow is determined. The law of flow assumes that the plastic strain is perpendicular to a plane. This law is defined as Equation (5):

$$d\varepsilon^p = \lambda \frac{\partial f(\sigma)}{\partial \sigma'} \quad (5)$$

Where λ is scalar and f (σ) is a level of stress function. If f (σ) is the same as the yield function, the related flow law holds. Otherwise, the law of flow will be unrelated, in which case, in addition to defining the yield function, a new function [g (σ)] will be defined, on which the plastic strain diagram will be perpendicular (Equation 6):

$$d\varepsilon^p = \lambda \frac{\partial g}{\partial \sigma'} \quad (6)$$

λ: is called the plastic coefficient, which in the elastic condition has a value of zero and in the plastic condition will have a value greater than zero. The general relationship between the effective stress diagram and the strain diagram can be expressed as Equations (7) and (8):

$$\sigma' = [D^e - \frac{\alpha}{d} D^e \frac{\partial g}{\partial \sigma'} \frac{\partial f^T}{\partial \sigma'} D^e]\varepsilon^0 \quad (7)$$

$$d = \frac{\partial f^T}{\partial \sigma'} D^e \frac{\partial g}{\partial \sigma'} \quad (8)$$

If the soil behavior is elastic, α is zero, and otherwise, α equals one. Also, f is the yield function, and g is the plastic potential level. If the Mohr-Coulomb Yield Criterion is, the Yield Criterion is defined as relations (9), (10) and (11):

$$f_1 = \frac{1}{2}\left|\sigma'_2 - \sigma'_3\right| + \frac{1}{2}(\sigma'_2 + \sigma'_3)sin\varphi - c.cos\varphi \geq 0 \quad (9)$$

$$f_2 = \frac{1}{2}\left|\sigma'_3 - \sigma'_1\right| + \frac{1}{2}(\sigma'_3 + \sigma'_1)sin\varphi - c.cos\varphi \geq 0 \quad (10)$$

$$f_3 = \frac{1}{2}\left|\sigma'_1 - \sigma'_2\right| + \frac{1}{2}(\sigma'_1 + \sigma'_2)sin\varphi - c.cos\varphi \geq 0 \quad (11)$$

The main parameters representing the Yield Criterion are the internal friction angle (φ) and soil cohesion (c), respectively. The shape of the function is conical in that the points inside it show the elastic range, and the border points show the plastic threshold. Since there is no related flow law in the Mohr-Coulomb Yield Criterion, the g function for the model is defined as a relation (12), (13), and (14):

$$g_1 = 1.2\left|\sigma'_2 - \sigma'_3\right| + 1.2(\sigma'_2 + \sigma'_3)sin\Psi \quad (12)$$

$$g_2 = 1.2\left|\sigma'_3 - \sigma'_1\right| + 1.2(\sigma'_3 + \sigma'_1)sin\Psi \quad (13)$$

$$g_3 = 1.2\left|\sigma'_1 - \sigma'_2\right| + 1.2(\sigma'_1 + \sigma'_2)sin\Psi \quad (14)$$

Parameter Ψ is used to model the volumetric strains of plastic in soils that increase in volume during cutting. Also, in the presence of cohesion, the Mohr-Coulomb model allows the element to be stretched, but in the modified Mohr-Coulomb Yield Model used in the program, the points under tension can be eliminated by defining complementary functions. These functions are defined as relations (15), (16), and (17):

$$f_4 = \sigma_1' - \sigma_t \geq 0 \quad (15)$$
$$f_5 = \sigma_2' - \sigma_t \geq 0 \quad (16)$$
$$f_6 = \sigma_3' - \sigma_t \geq 0 \quad (17)$$

At new levels, it is assumed that the related law is in place. If the stress range is within the yield function, the body behavior will be a function of the linear hook model. According to what has been said, in this model, the stress-strain relationship is defined by defining 5 parameters that can be achieved by known and common experiments in soil. These parameters are soil shear modulus, Poisson's ratio, friction angle, cohesion, and expansion angle, which are formulated in equilibrium and compatibility equations in each of the elements by assuming planar strains and are determined by gradually applying loads and comparing them with yielding levels. (Zienkiewicz, et al., 1977) [21].

2.3. MODELING AZADI DAM IN ABACUS SOFTWARE

Abaqus is a set of highly powerful finite element modeling programs capable of solving simple to complex linear analysis and nonlinear modeling problems. In the nonlinear analysis, Abaqus automatically selects the values of the convergence tolerances and also adjusts their values during the analysis to obtain the correct answer. As a result, the user rarely has to specify the values of the numerical solution control parameters. It also supports Python open-source programming language for programming within the software. The ability to write scripts in software doubles its modeling capabilities. In this research, Abaqus has been used to calculate the stress and strain pressure, assuming the flat strain behavior in Azadi Dam. For this purpose, the largest section of the dam has been modeled using Abaqus software and analyzed with eight-node elements [22]. Figure 2 shows the modeling and meshing of the Azadi Dam.

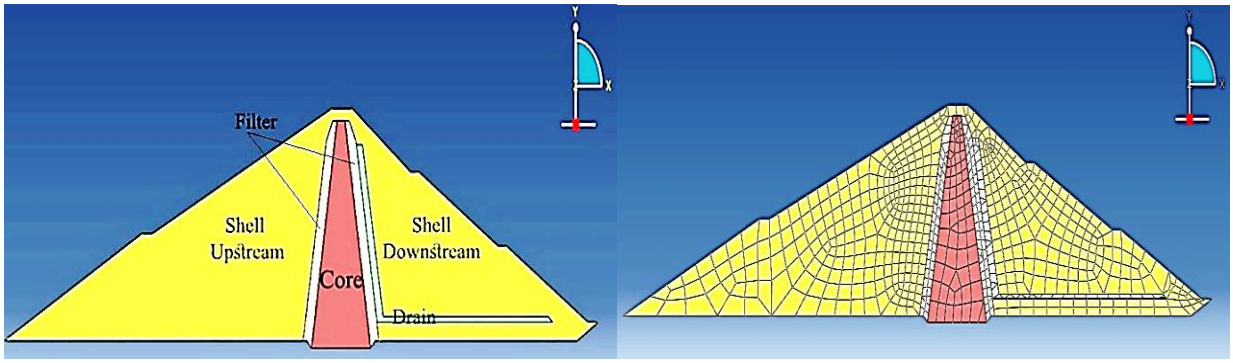

Figure 2. Modeling and meshing of Azadi Dam in Abacus software

For dynamic analysis, it is first necessary to perform quasi-static analysis, and after equilibrium, dynamic analysis started. The damping used in the dynamic analysis of the Azadi Dam is of the Rayleigh Damping type. Rayleigh Damping is the most common type of mechanical damping used in dynamic analysis. Rayleigh Damping is generally used in time-dependent applications to provide attenuation that is almost independent of frequency. The damping percentage is considered equal to 1% due to the elastoplasticity of the behavioral model of the materials. In behavioral models that allow the soil to enter the plastic part (Mohr-Coulomb), considering the energy dissipation capability in the model, it is reasonable to include damping between 0 and 1%. In fact, for most dynamic analyzes that involve large strain conditions, only a small percentage of damping is required. To evaluate the performance and seismic design of dams against earthquakes, the force caused by the earthquake should be suitably applied to the dam structure, and the seismic responses of the dam should be calculated by performing nonlinear analysis. Since the Azadi Dam site is located on the Shale rock foundation, the location of the accelerometer must be consistent with the geological conditions of the site. Therefore, for the dynamic analysis of Azadi Dam, the accelerometers of earthquakes have been selected that have been recorded on rocks or rocks with a shear velocity of less than 760 m/sec. It should be noted that the accelerometers have been selected based on the type of soil at the station (soil II). For this purpose, the soil of the stations in question has been determined based on geophysical methods. Based on seismicity studies in the area of the Azadi Dam construction site, the values of design basis seismicity parameters (DBL), design top (MDL), and maximum acceptability (MCL) are 0.20, 0.30, and 0.51, respectively, for maximum horizontal acceleration and 0.12. , 0.20 and 0.34 were estimated for the maximum vertical acceleration, and the maximum earthquake occurred in the region with a magnitude of 7 (Abdan Faraz Consulting Engineers). In the study site, the earthquake coefficient has been determined and selected for stability analysis of 0.17 (equivalent to one-third of the maximum tolerated earthquake, based on Pyke's recommendation). Limiting the maximum acceleration of the input stimulus is 0.17 g due to the dynamic analysis of moderate and weak earthquakes by accepting low error

and assuming linear soil behavior. It can also be related to the avoidance of unrealistic tensile stresses in the lower shell elements, which occurred after adding dynamic to quasi-static stresses in earthquakes larger than 0.17 g due to the use of the linear behavior assumption. Assuming the true nonlinear behavior of the soil and the inability to withstand the aggregates' tensile strength, this problem can be solved. Therefore, to perform dynamic analysis and generate the input stimulus, the Tabas earthquake accelerometers with a maximum acceleration of 0.83 g and a time of 33 seconds have been used with the idea (Table 1 and Figure 3).

Table 1. Earthquake characteristics used in dynamic analysis of Azadi Dam

Earthquake	Maximum acceleration (g)	Maximum velocity (m/sec)	Maximum Horizontal displacement(m)	Time (sec)
Tabas	0.83	0.97	0.38	16.42

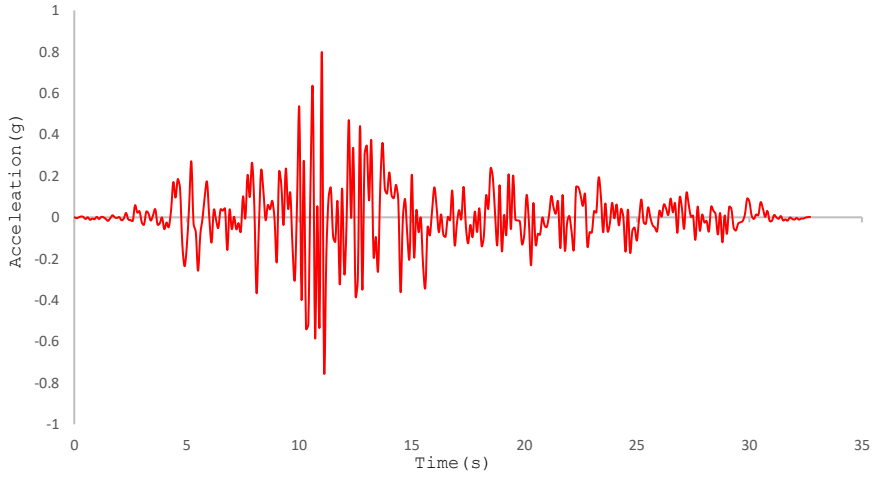

Figure 3. Accelerometer used in dynamic analysis of Azadi Dam (Tabas earthquake)

In Table 2, the characteristics of Marvak dam materials are presented for use in numerical modeling.

Table2. Initial values of mechanical parameters of the building materials and dam body, instrument report of Azadi Dam (2012)

Material	Model: Mohr-Coulomb	Type Material	γ (kN/m3)	K0	E (MPa)	ν	c (kN/m2)	φ (○)
Core	Elasto-plastic	Undrained	20.1	0.72	27.5	0.42	100	21
		Drained				0.35	90	30
Shell	Elasto-plastic	Drained	21.8	0.47	70	0.31	-	38
Filter	Elasto-plastic	Drained	21.2	0.54	35	0.28	-	32
Drain	Elasto-plastic	Drained	21.7	0.52	45	0.26	-	35
Foundation	Elasto-plastic	Drained	25.3	0.33	2600	0.20	1080	28

3. RESULTS AND DISCUSSION

In this research, the studied model is Azadi Dam in Kermanshah province, which has been modeled with Abaqus finite element software. The modeling of vertical and horizontal displacements has been done by two methods of quasi-static and dynamic analysis. Besides, dynamic analysis has been performed in the case of a full reservoir (steady-state).

3.1. ANALYSIS SETTLEMENT IN THE QUASI-STATIC METHOD

As can be seen in Figure (4), the maximum settlement of 43.2 cm occurred at the top level of the dam and then decreased downwards and in a certain order by 3.5 cm. The reason for this behavior is the compaction and consolidation of the lower layers due to the weight of the higher layers. Also, due to the fineness of the core material, the difference between the layers inside the core is much less than other areas of the dam.

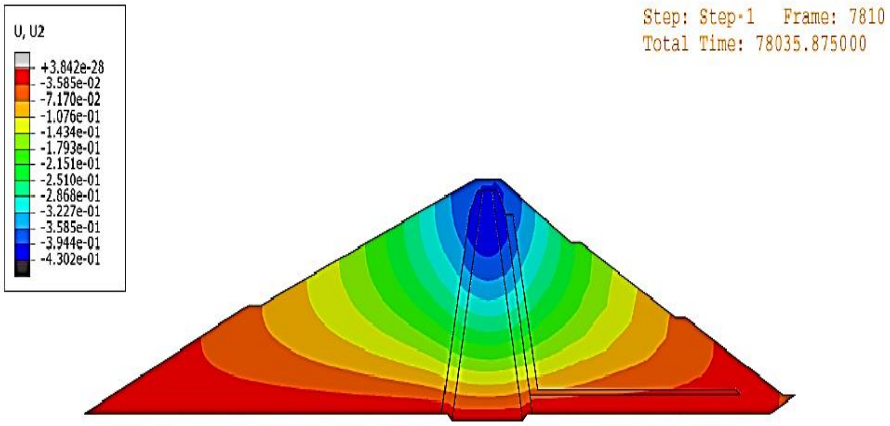

Figure 4. Quasi-static analysis of the settlement, Azadi earth dam

3.2. ANALYSIS OF VERTICAL AND HORIZONTAL DISPLACEMENTS IN THE DYNAMIC METHOD

Figure (5) shows the horizontal displacements of the Azadi Dam. Most horizontal displacements occurred after the application of seismic force in the upper levels and near the crest of the dam. The amount of horizontal displacements in the dynamic analysis is 34 cm, which has decreased from the upper levels of the core to the lower levels. The decreasing trend of horizontal displacements is more observed in the downstream shell than in the upstream shell. The results show that the average shell horizontal displacements downstream are 22 cm and in the upstream18 mm. Also, the horizontal displacement of the dam is towards the lake. In general, the instability of the dam during the earthquake is in the form of settlement of the dam crest and swelling of the downstream parts towards the lake reservoir, which is naturally acceptable.

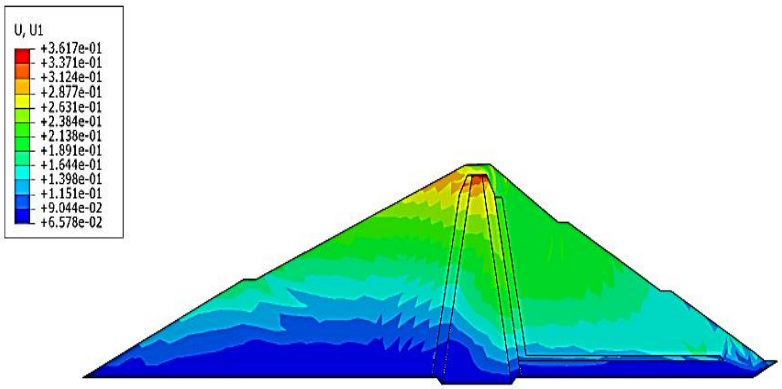

Figure 5. Dynamic analysis of horizontal displacement, Azadi earth dam

As shown in Figure (6), the maximum amount of settlement after the application of seismic force occurred in the upper levels of the dam and specifically in the upstream crust, and its value is equal to 68 cm. The reason is that the cavities disappear after the earthquake, and the coarse-grained materials get closer to each other, and the amount of crust settlement has decreased with an angle of about 40 degrees downstream. It should be noted that the rate of reduction of settlement in the upstream shell is slower than the downstream shell.

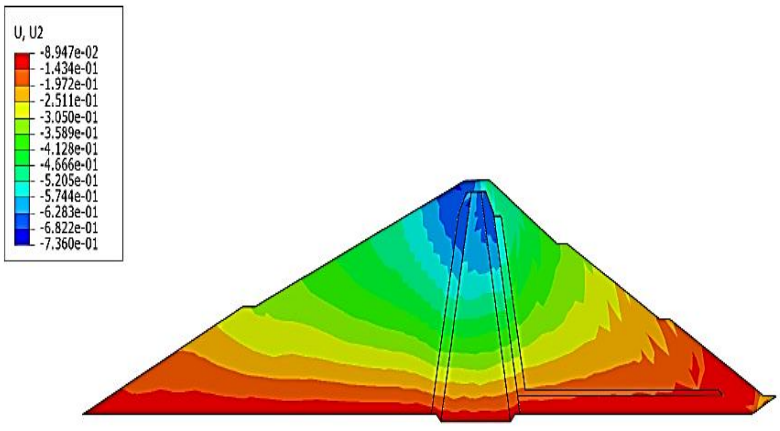

Figure 6. Dynamic analysis of settlement, Azadi earth dam

According to Figures (7) and (8), three levels of the floor (EL.1265 masl), middle (EL.1285 masl), and upper (EL.1310 masl) of the body have been used to extract the diagrams of the settlement diagram upstream of the Azadi Dam, considering the full reservoir

.

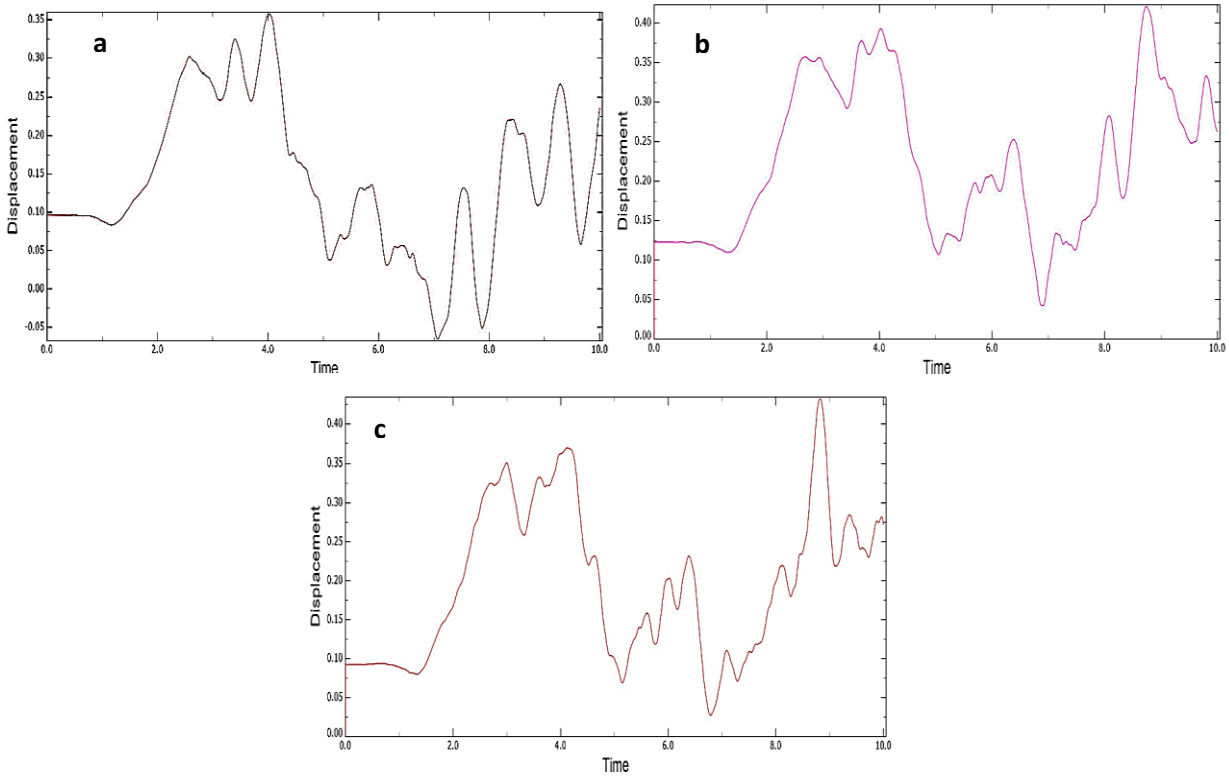

Figure 7. Dynamic analysis of horizontal displacement of the upstream shell of Azadi Dam, a: EL.1265 masl, b: EL.1285 masl, c: EL.1310 masl

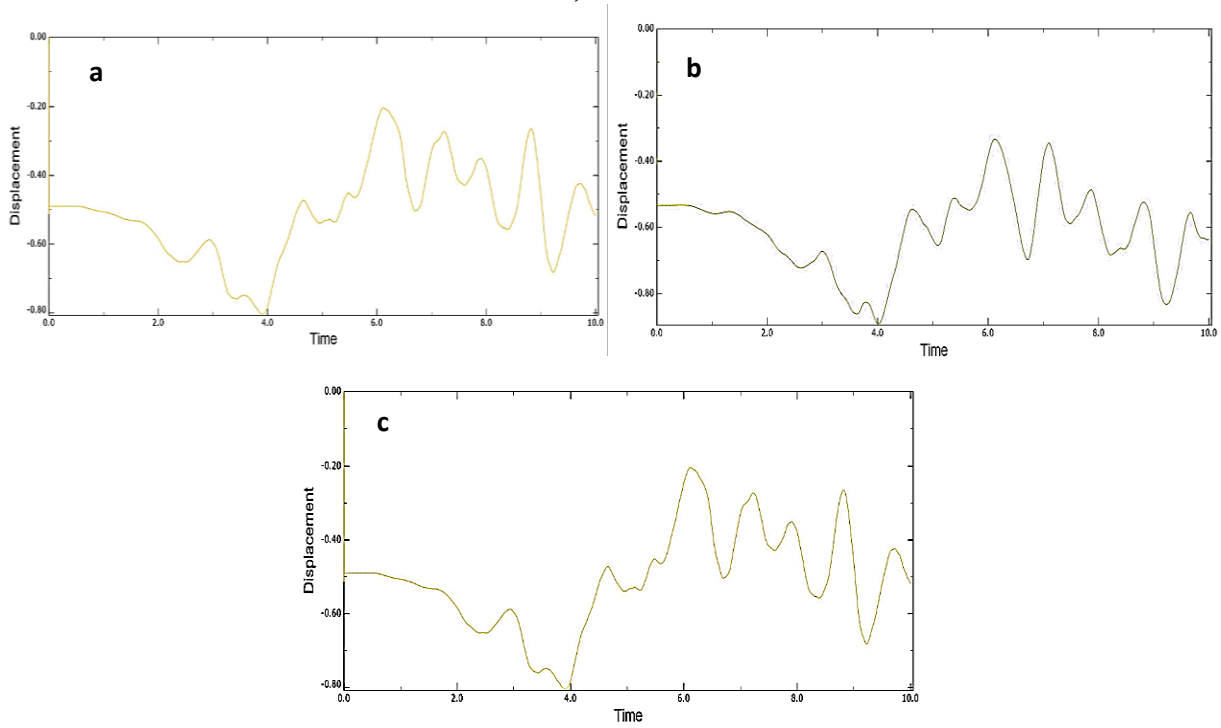

Figure 8. Dynamic analysis of settlement of the upstream shell of Azadi Dam, a: EL.1265 masl, b: EL.1285 masl, c: EL.1310 masl

As shown in Figures (7) and (8), the most horizontal displacement and settlement occurred at the highest level of the dam. In horizontal displacement, the changes are relatively uniform for up to 1.8 seconds, after which the displacements change in a positive direction and with a large slope. Then, due to the spatial period of the earthquake, a small amount returned in a negative direction and finally reached equilibrium after the tremor. The settlement was almost constant until 0.5 seconds, after which the settlement increased with a relatively steep slope. It should be noted that during an earthquake, the settlement is more sensitive to horizontal displacement, so that settlement is 66% higher in the upper levels of the crust, 55% in the middle of the dam, and 52% at the bottom of the crust. The interpretation

of Figures (7) and (8) is in the form of Table (3).

Table.3. Horizontal and vertical displacements of the upstream shell of Azadi Dam

Maximum settlement (cm)	Maximum settlement time (s)	Maximum horizontal displacement (cm)	Maximum horizontal time (s)	Area
80	3.9	35	4.1	floor (EL.1265 masl)
90	3.85	41	8.6	middle (EL.1285 masl)
97	3.8	43	8.75	upper (EL.1310 masl)

As can be seen in Figures (9) and (10), most horizontal and vertical displacement (settlement) occurred above the clay core.

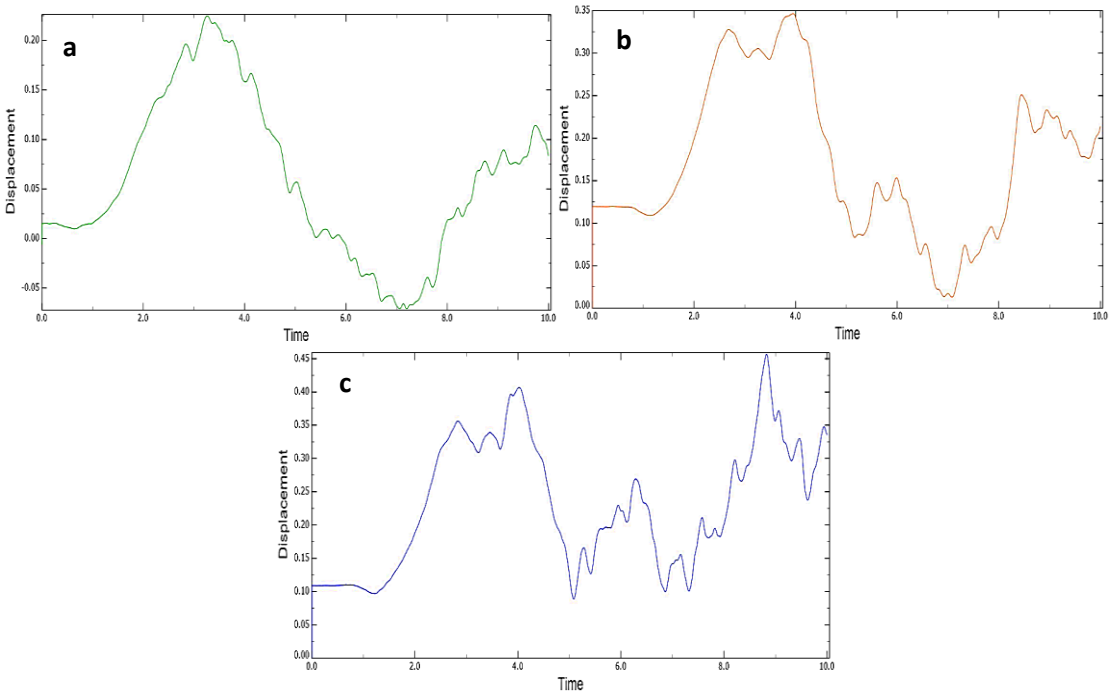

Figure 9. Dynamic analysis of horizontal displacement of the core of Azadi Dam, a: EL.1265 masl, b: EL.1285 masl, c: EL.1310 masl

At the high level of the dam core and up to 0.3 seconds, the displacements are observed with small changes over time, then we will have displacements in both directions with a high slope, and it has reached the maximum value. This is due to the high magnitude of the earthquake with a time interval of 4 seconds. The displacement then changes direction to reach equilibrium eventually. This oscillating motion is due to the force of the earthquake.

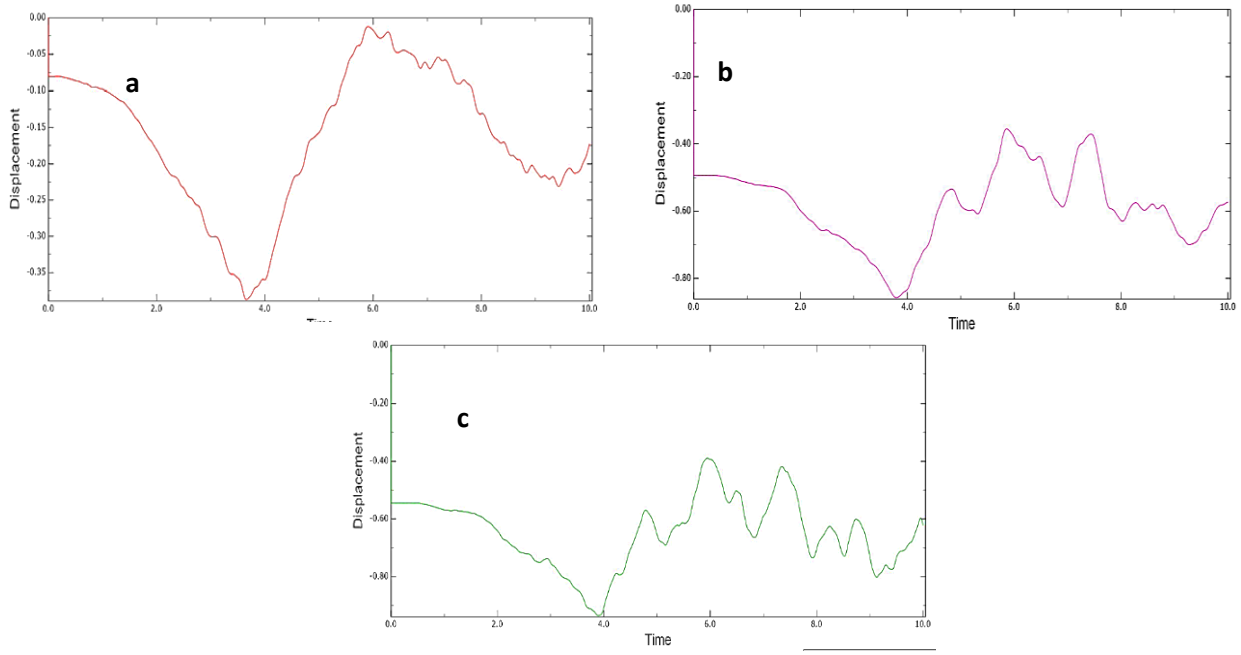

Figure 10. Dynamic analysis of settlement of the core of Azadi Dam, a: EL.1265 masl, b: EL.1285 masl, c: EL.1310 masl

The interpretation of Figures (9) and (10) is in the form of Table (4).

Table.4. Horizontal and vertical displacements of the core of Azadi Dam

Maximum settlement (cm)	Maximum settlementtime (s)	Maximum horizontal displacement (cm)	Maximum horizontal time (s)	Area
33	3.6	28	3.5	floor (EL.1265 masl)
81	5.8	35	3.9	middle (EL.1285 masl)
95	3.8	46	8.7	upper (EL.1310 masl)

4. CONCLUSION

The results of the dam settlement in the dynamic analysis are 37% higher than the quasi-static session. With the increasing stiffness of materials, horizontal and vertical displacements in the dam have decreased. The highest amount of settlement in both quasi-static and dynamic states occurs at the upper levels of the dam, with the difference that in the dynamic state and under full reservoir conditions, the upstream shell is more affected by settlement. During an earthquake, the settlement is more sensitive to horizontal displacement, so that settlement at the upper levels of the crust is 66%, the middle 55%, and the bottom 52% more than the horizontal displacement. The rate of settlement reduction is faster in the downstream shell than in the upstream so that it is 22 cm downstream and 18 cm upstream.

FUNDING/SUPPORT

Not mentioned any Funding/Support by authors.

ACKNOWLEDGMENT

Not mentioned by authors.

AUTHORS CONTRIBUTION

This work was carried out in collaboration among all authors.

CONFLICT OF INTEREST

The author (s) declared no potential conflicts of interests with respect to the authorship and/or publication of this paper.

5. REFERENCES

[1] Ambraseys NN, Sarma SK. The response of earth dams to strong earthquakes. Geotechnique. 1967 Sep;17(3):181-213. [View at Google Scholar] ; [View at Publisher]

[2] Sarma SK. Seismic stability of earth dams and embankments. Geotechnique. 1975 Dec;25(4):743-61. [View at Google Scholar] ; [View at Publisher]

[3] Tsai PH, Hsu SC, Lai J. Effects of core on dynamic responses of earth dam. InSlope Stability, Retaining Walls, and Foundations: Selected Papers from the 2009 GeoHunan International Conference 2009 (pp. 8-13). [View at Google Scholar] ; [View at Publisher]

[4] Tsompanakis Y, Lagaros ND, Psarropoulos PN, Georgopoulos EC. Simulating the seismic response of embankments via artificial neural networks. Advances in Engineering Software. 2009 Aug 1;40(8):640-51. [View at Google Scholar] ; [View at Publisher]

[5] Elia G, Amorosi A, Chan AH, Kavvadas MJ. Numerical prediction of the dynamic behavior of two earth dams in Italy using a fully coupled nonlinear approach. International Journal of Geomechanics. 2011 Dec 1;11(6):504-18. [View at Google Scholar] ; [View at Publisher]

[6] Mukherjee S. Seismic slope stability analysis of earth dam: Some modern practices. Int. J. Recent Adv. Mech. Eng.. 2013;2(1):41-50. [View at Google Scholar] ; [View at Publisher]

[7] Huang LJ, Sheen YN, Hsiao DH, Le DH. Quasisteady analysis of excavation backfilled with soil-based controlled low-strength material using finite element and boundary element methods. Inthe International Conference on Green Technology for Sustainable Development 2014 (pp. 30-31). [View at Google Scholar] ; [View at Publisher]

[8] Panulinová E, Harabinová S. Methods for analyzing the stability of an earthen dam slope. InAdvanced Materials Research 2014 (Vol. 969, pp. 245-248). Trans Tech Publications Ltd. [View at Google Scholar] ; [View at Publisher]

[9] Bandini V, Biondi G, Cascone E, Rampello S. A GLE-based model for seismic displacement analysis of slopes including strength degradation and geometry rearrangement. Soil Dynamics and Earthquake Engineering. 2015 Apr 1;71:128-42. [View at Google Scholar] ; [View at Publisher]

[10] Luo J, Zhang Q, Li L, Xiang W. Monitoring and characterizing the deformation of an earth dam in Guangxi Province, China. Engineering Geology. 2019 Jan 8;248:50-60. [View at Google Scholar] ; [View at Publisher]

[11] Sukkarak R, Jongpradist P, Pramthawee P. A modified valley shape factor for the estimation of rockfill dam settlement. Computers and Geotechnics. 2019 Apr 1;108:244-56. [View at Google Scholar] ; [View at Publisher]

[12] Zhang JM, Yang Z, Gao X, Zhang J. Geotechnical aspects and seismic damage of the 156-m-high Zipingpu concrete-faced rockfill dam following the Ms 8.0 Wenchuan earthquake. Soil Dynamics and Earthquake Engineering. 2015 Sep 1;76:145-56. [View at Google Scholar] ; [View at Publisher]

[13] Rashidi M, Heidar M, Azizyan G. Numerical analysis and monitoring of an embankment dam during construction and first impounding (case study: Siah Sang Dam). Scientia Iranica. 2018 Apr 1;25(2):505-16. [View at Google Scholar] ; [View at Publisher]

[14] Gikas V, Sakellariou M. Horizontal deflection analysis of a large earthen dam by means of geodetic and geotechnical methods. In13th FIG international symposium on deformation measurements and analysis and 4th IAG symposium on geodesy for geotechnical and structural engineering 2008 May 12. [View at Google Scholar] ; [View at Publisher]

[15] Silvani C, Bonelli S, Philippe P, Désoyer T. Buoyancy and local friction effects on rockfill settlements: a discrete modelling. Computers & Mathematics with Applications. 2008 Jan 1;55(2):208-17. [View at Google Scholar] ; [View at Publisher]

[16] Karalar M, Çavuşli M. Evaluation of 3D Nonlinear Earthquake Behaviour of the Ilısu CFR Dam under Far-Fault Ground Motions. Advances in Civil Engineering. 2019 Jan 1;2019. [View at Google Scholar] ; [View at Publisher]

[17] Karalar M, Cavusli M. Examination of 3d long-term viscoplastic behaviour of a CFR dam using special material models. Geomechanics and Engineering. 2019;17(2):119-31. [View at Google Scholar] ; [View at Publisher]

[18] Karalar M, Cavusli M. Seismic effects of epicenter distance of earthquake on 3D damage performance of CG dams. Earthquakes and Structures. 2020;18(2):201-13. [View at Google Scholar] ; [View at Publisher]

[19] Kartal ME, Cavusli M, Sunbul AB. Assessing seismic response of a 2D roller-compacted concrete dam under variable reservoir lengths. Arabian Journal of Geosciences. 2017 Nov 1;10(22):488. [View at Google Scholar] ; [View at Publisher]

[20] Azadi Reservoir Dam Design, Studies of the second phase, seismicity and earthquake engineering of Abdan Faraz Consulting Engineers, West Regional Water Company, 2003. [View at Publisher]

[21] Zienkiewicz OC, Taylor RL, Zienkiewicz OC, Taylor RL. The Finite Element Method (McGrawHill, London). [View at Google Scholar]

[22] ABAQUS Theory Manual, version 6.11-3., 2011. Dassault Systems. [View at Publisher]